METHODS OF VENUS RADIOLOCATION MAP SYNTHESIS USING STRIP IMAGES OF VENERA-15 AND VENERA-16 SPACE STATIONS

I. BOCKSTEIN, P. CHOCHIA, and M. KRONROD

Institute for Information Transmission Problems, USSR Academy of Sciences, Moscow, U.S.S.R.

(Received 21 September, 1988)

Abstract. The methodology and the results of Venus northern hemisphere (approximately to 30°N) map synthesis are described. The synthesis was carried out in the Institute for Information Transmission Problems of the USSR Academy of Sciences using the data of strip survey of Venus surface received from VENERA-15 and VENERA-16 space stations. Interactive image processing system of the institute was used for this purpose. The problem of map synthesis was divided into four stages – pre-processing of about 300 strips images available, geometrical transformation of the strips and the synthesis of so-called sectors from 10–16 strips, joining all the 19 sectors into 34 map sheets and filling the polar area in the middle of the central sheet. The main mode of work in the course of map synthesis was the interaction of the operator with the system. This enabled to achieve high accuracy of strips referencing, indistinguishability of the borders between strips and sectors, the absence of false objects, and, as a result, high visual quality of the map.

1. Introduction

From October 1983 to July 1984 the side-looking radio-location of Venus surface was carried out by the Soviet space stations VENERA-15 and VENERA-16. Information transferred to the Earth was enough to produce radiolocation map of Venus Northern area approximately up to 30°N (Bogomolov *et al.*, 1985; Kuzmin, *et al.*, 1986).

The space stations moved along the elliptic orbits inclined to Venus axis at about 2.5°. The minimum distance of stations from the planet surface was about 1000 km, the maximum distance being 65 000 km (Figure 1a). The circulation period of each station was 24 h. The station carried the side-looking radar with synthetized aperture. This radar (Bogomolov *et al.*, 1985) was designed by the Moscow Energy Institute. When flying near the pericentre, the radar scanned from the height of 1000–2000 km a surface strip of about 150 km wide and 6000–7000 km long; this strip was oriented along the flight direction (Figure 1b). Due to the planet's rotation (at the angle of 1.48° during each 24 h) the position of the strips on its surface changed from circuit to circuit; the parameters of the orbits and of the radars were chosen in such a way that two images consecutively formed had a small overlap at the end of location (see Figure 4b). As a result, after Venus full revolution cycle the information about the significant part of its Northern hemisphere (roughly from 30° to 88°N) was received. After special turn of stations and radar antennas (see Section 4) it became possible to obtain the images of the strips passing through Venus North pole.

Earth, Moon, and Planets **43** (1988) 233–259.
© 1988 *by Kluwer Academic Publishers.*

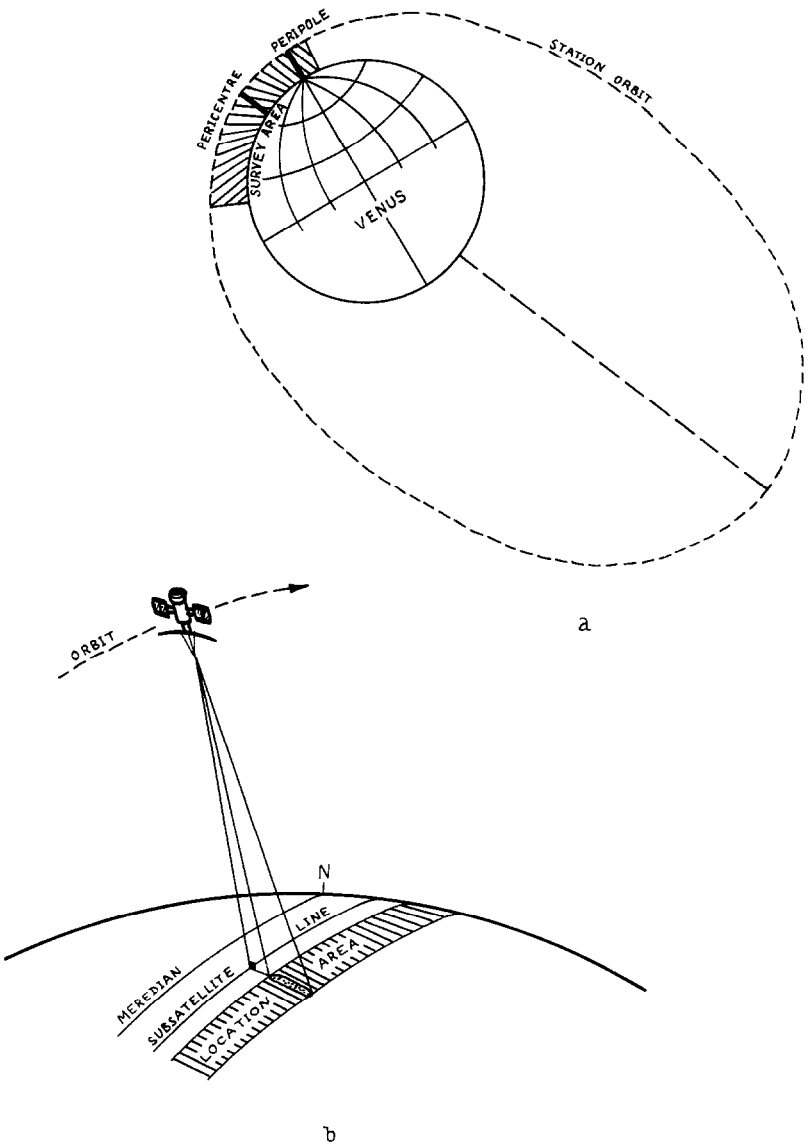

Fig. 1. a – the layout of station flight; b – the layout of surface surveying.

The stations surveyed the Venus surface in two modes – the strip mode and the frame mode that differed in the technique of information obtaining and processing. When using strip mode (the data of which were used in our work) the equipment mounted in each station formed the strip image in real time by the sequential extraction and eightfold superposition of strip transverse lines in three frequency (Doppler) channels (Bogomolov *et al.*, 1985). The resolution of the strip mode was 2–3 km/pixel depending on the flight height.

Strip images transmitted from the stations to the Earth consisted of 2500–3000 lines united in pairs and provided with a number. The line contained three consecutive records with 63 elements; they corresponded to three Doppler channels. The brightness value for each element was represented by 12-bit code and could range from 0 to 4095. The method of obtaining strip images and the stations' great distance from the Earth resulted in various kinds of distortion on these images (Figure 2); it was necessary to compensate all distortions before the beginning of the map synthesis from separate strips.

(1) The automatic gain control was used in the course of strips formation aboard the stations. Therefore, the gain factor changed from one line of the strip to another one. This led to changes in line contrast and, consequently, to the emergence of the line structure at the image.

(2) The strong irregularity of the radar antenna diagram resulted in the considerable attenuation of the signal near the strip edges (this led to the emergence of a dark zone at the image).

(3) The change of the flight height during the survey led to the determined variation in the phase increment, i.e. to the cyclic shift of information in each

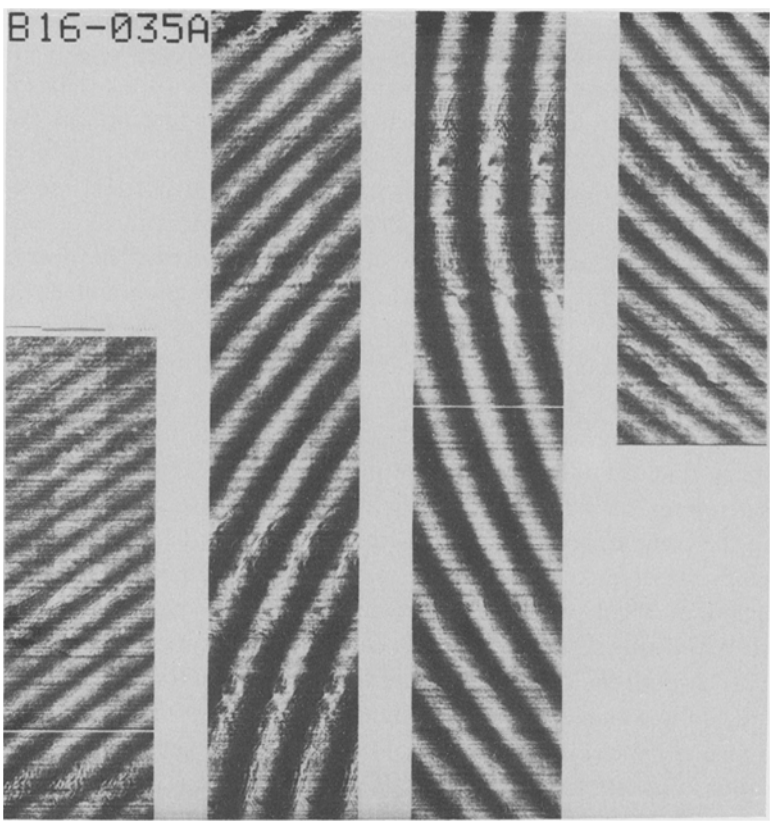

Fig. 2. An image of strip before pre-processing.

Doppler channel of each image line. As a result, the dark zone described on page 2 was bent with respect to the strip direction.

(4) The variations of the height of Venus relief resulted in additional random phase changes and in additional cyclic shift of information.

(5) Noise in Venus-Earth communication channel often led to the disappearance of some lines or to considerable lines distortions.

(6) The use of side-looking radar with synthetized aperture determined the presence of speckle noise in each Doppler channel.

In 1984–1986 Venus Northern area map was synthetized out of the strip images in the Institute for Information Transmission Problems of the USSR Academy of Sciences. The interactive image processing system of the institute (Kronrod and Chochia, 1983) was used for this purpose. This sytem incorporates the 16-bit mini-computer Alpha 16 with 160 Kbites of core memory and a speed of about 300 000 operations per second, fast floating point processor, magnetic discs with overall capacity of 10 Mbites, digital tape recorders and some standard external devices, as well as image input/output device that enables one to record the results of work on a film, and the display processor (Bockstein, 1981). The latter is a special device ensuring the interaction of operator with images. It can be used to store two images containing 256 lines by 512 elements with 256 brightness levels. The display processor includes a high-speed arithmetic device that gives possibility to carry out many image processing operations (e.g., to form the difference or the sum of two images, to change their contrast, to superimpose images etc.) in real time.

The base of system software is an interactive operating system created at the Institute for Information Transmission Problems (Kronrod and Chochia, 1983). It effectively implements various methods of image processing. The operator interacts with the system through answers to questions put by programs in the natural language and through the use of dialogue opportunities of the display processor. This minimizes the requirements of the operator's special training and enables the elaboration of effective technological instructions to solve specific problems.

The final aim of the work performed was to prepare a map of Venus Northern area in the normal azimuthal equidistant projection. This projection (chosen out of the considerations of reducing the complexity of geometrical transformation and of raising the comparability of source strip images with the images of these strips on the map) preserves the scale along the planet's meridians (and actually along the direction of flight, as the inclination of orbit is small enough). The scale along the parallels increases as $\varphi/\sin\varphi$ when the latitude $90° - \varphi$ decreases. Taking into account the size of strips and their real resolution, the scale of the map in polar region was chosen equal to 2.5 km pixel^{-1}; so that the map (see Figure 13) had a diameter of about 6000 pixels. Taking into account some technological considerations and the limited capacity of discs available (2.5 Mbite per disc), the map was divided into 49 square sheets; each of them was 1024×1024 pixels

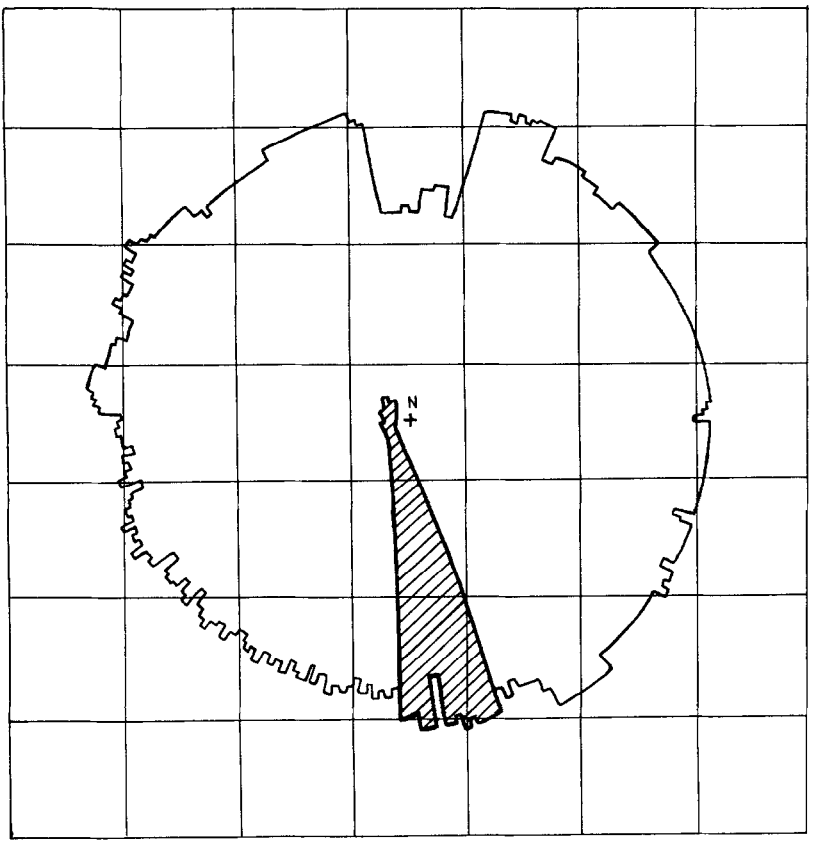

Fig. 3. The layout of the map divided into sheets (shaded area corresponds to sector 1).

in size. The middle of the central sheet corresponded to Venus North pole (Figure 3). Only 34 of these sheets contained information from the strip survey.

The data received were processed and the map was synthetized as follows. The initial information about each strip was first of all fed into the system. Then the strips were preprocessed to eliminate the distortions described above. After this the strips consecutively obtained were transformed into the map format and joined into groups (sectors) comprising up to 16 strips. Nineteen sectors synthetized this way were turned at proper angles, and the sheets of the map were formed from them (Figure 4a, b). A special procedure was used to fill the polar area (a specific location mode was employed for this area, and a special type of strips transformation was therefore necessary). The strips passing through the pole were joined with the image of map central sheet.

In the subsequent sections of this paper the procedures of strips pre-processing, sectors synthesis, map sheets formation and solar area filling will be described in more detail.

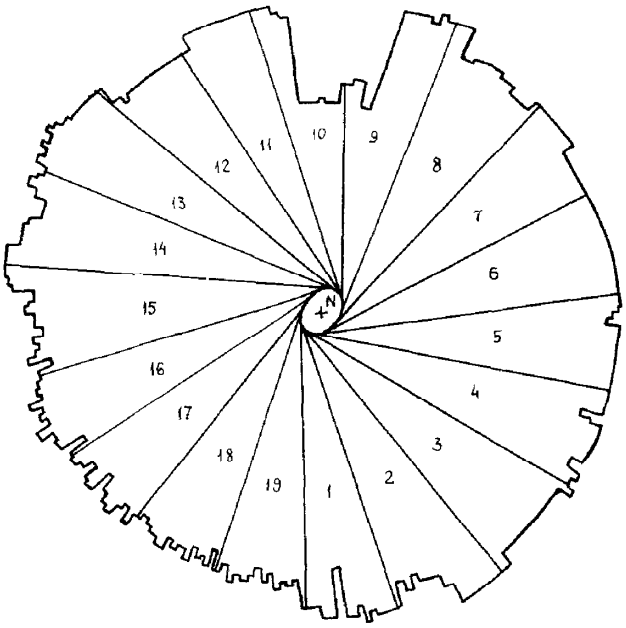

a

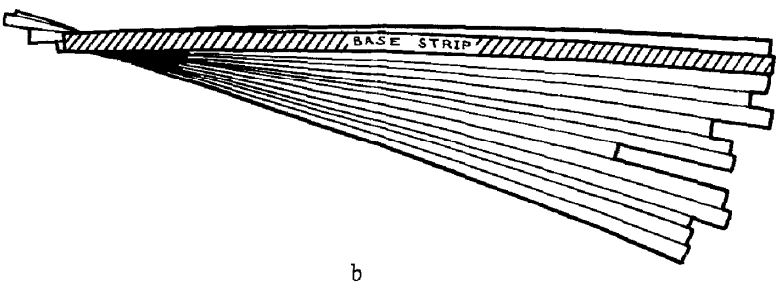

b

Fig. 4. a – the composition of the map from the sectors; b – the composition of sector from the strips.

2. Strip Pre-processing

The data obtained in the course of the strip survey of Venus surface were received by the Institute for Information Transmission Problems as records on magnetic tapes. Initially a tape contained, as a rule, the results of a single survey. Then a more compact record format was introduced. As a result, it became possible to record onto each tape the information about a few days of survey; data of each strip were stored in individual file whose header contained the information about survey

data and location mode. Because of the great volume of initial data (about 300 strip images were formed during the stations' flight) the systematic registration of these data was organized since the very beginning of work. After feeding each strip image in the image processing system it was supplied with serial number of the input and with the identification number in the form of B-XX-YYY-Z, where YYY = 1–269 – the serial number of the survey day (YYY = 1 corresponded to October 16, 1983), XX = 15 or 16 – station number, Z = A or B – equipment unit used during location.

As a result of the input the strip was divided into four parts and was recorded on the magnetic disc as a square image with 1024 × 1024 pixels (Figure 2).

Along with strips input the data on the parameters of stations orbits during the survey were also fed into the system. The input catalogue created specially for this purpose included for each strip the information on its serial and identification numbers, on the station energy in the appropriate orbit circuit, E, on the flight height at the pericentre point, H_{pc}, on the orbit inclination, φ_{pp}, and on the number of line corresponded to the peripole, r_{pp} (this information was found from the trajectory measurements carried out by the Institute of Applied Mathematics of the USSR Academy of Sciences (Akim *et al.*, 1986)). The data on the biquadratic approximation of working part of orbit – the number of line that corresponded to the pericentre, r_{pc}, the initial phase, a, the quadratic, b, and biquadratic, c coefficients, and coordinates of the beginning and the end of the strip were also introduced into the catalogue. (The method of obtaining these data and their meaning are given below.) The data of the catalogue were used in the course of the geometric transformations of strips before synthetizing the sectors. Since some of the orbital data for a number of strips were absent or for some reasons quite incorrect, the catalogue was edited in the course of its filling. As a rule, editing was performed through interpolation. Sometimes coarser empirical methods were also used; they were based on the assumptions that the station energy varied very slowly, the height of the flight changed smoothly in the periods between trajectory corrections, and the law of varying the orbit inclination was close to the sinusoidal one. All changes of the catalogue content were made, of course, before the beginning of using the changed data.

After the input of initial strip image of Figure 2 from the tape it was preprocessed to correct the distortions described in the Introduction. The first preprocessing step included the correction of multiplicative distortions introduced by the automatic gain control. The correction was performed according to the formula

$$y_{ij} = \left(3 \times 10^4 / \sum_{k=1}^{K} x_{ik}\right) x_{ij} \tag{1}$$

(where x_{ij} and y_{ij} denote hereafter the brightness values of pixels of initial and processed image, respectively; i, the line number; j, number of element in this line). Since, as mentioned above, the length of the line for each Doppler channel was equal to 63 elements, the value of K was taken as $3 \times 63 = 189$. The constant 3×10^4 was chosen experimentally as ensuring sufficient dynamic range of image

and the absence of distortions. The result of the transformation (1) (Figure 5b) was presented in the 8-bit format. The brightness of each element of the corrected strip could assume the values of 1–255. The value 0 was given beforehand for indicating the background part of strips and sector images. This gave possibility to simplify appreciably the synthesis procedures described in Sections 2, 3, and 4.

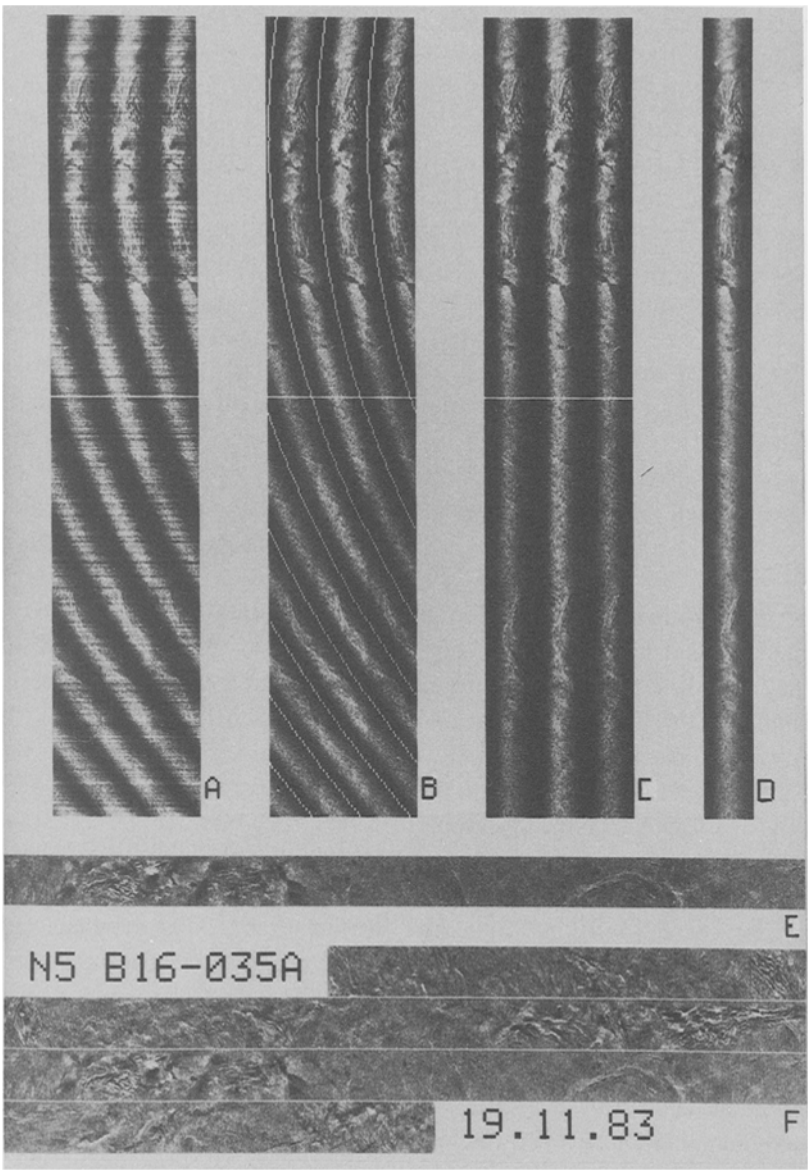

Fig. 5. Pre-processing stages: a – a fragment of initial strip image; b – the result of correcting the distortions caused by automatic gain control; c – the result of phase correction; d – the result of Doppler channels averaging; e – the result of antenna diagram nonuniformity correction; f – the whole strip image after pre-processing.

When line nonuniformity of strip images was corrected, the geometrical correction of this image was used to compensate the phase increment due to the change of the station flight height. For this purpose the lines of each Doppler channel were cyclically shifted so that the brightness minimum corresponding to the minimal antenna sensitivity (the dark zone in Figure 5a, b) should get to the edge of image for this channel. After some experiments we saw that the regular change in the flight height (and the curvature of the dark zone) was well described by the bi-quadratic polynomial of the type

$$\omega(i) = a + b(i - r_{pc})^2 - c(i - r_{pc})^4, \tag{2}$$

where r_{pc} stands for the line number corresponded to the pericentre (i.e. to the minimal flight height). The coefficients a, b, c, as well as r_{pc} value were chosen by the operator in the interactive mode. For each set of the values of these parameters a line was drawn on the strip image at the screen of the display processor. This line was given by the polynomial (2) taken modulo 189 (the whole width of strip image). Using the method of serial approaches, the operator altered the parameters a, b, c, and r_{pc} until the line coincided with the middle of the dark zone along the whole strip (see Figure 5b). Upon reaching this result the parameters found were recorded in the catalogue while the image was transformed by a formula

$$y_{ij} = x_{(i - \omega(i))_{\mathrm{mod}\,63}, j} \tag{3}$$

for the left-hand Doppler channel, and by similiar formulae for two other channels. Due to the correction of the phase increment the strip image became straight as shown in Figure 5c.

The next step of preprocessing was the compensation for the malfunctions due to the low signal-to-noise ratio in Venus-Earth communication channel. As a rule, these malfunctions resulted in the complete disappearance of some strip lines. In the case of disappearance of more than four lines in succession they had to be replaced by neighbouring ones. (Shorter intervals were filled in the course of channels averaging.)

A single image (Figure 5d) was formed through averaging of all the three Doppler channels that did not contain gross malfunctions. The following formula was used for this purpose:

$$y_{ij} = (x_{ij} + x_{i-2,j+63} + x_{i-4,j+126})/3. \tag{4}$$

The averaging resulted in an essential reduction of speckle noise. Since for the operating range of flight heights the lines of neighbouring channels whose numbers differ roughly by 2 (actually by 1.5 to 2.5) correspond to the same part of Venus surface the image sharpness did not decrease after averaging by formula (4). If the lines of one or even two channels were malfunctioned, they were not used in averaging. Due to the shift between the channels this mode of the operation led to the restoration of image areas where the initial strip had malfunctions with the length of up to four lines (cf. Figure 5c and Figure 5d).

Further preprocessing consisted in additional correction of random phase changes due to local relief of Venus surface. (The above-mentioned correction by formula (3) compensated only the slow changes of phase due to the ellipticity of the orbit.) As previously, the aim of correction procedure was to place the brightness minimum caused by the decrease of antenna sensitivity to the edge of the strip. In fact, from Figure 6, it is clear that when the relief height h varies, the position of this minimum is shifted approximately by $h \cdot tg\alpha$. At $\alpha = 12°$ and with the maximum height of Venus relief of about 12 km this value is roughly 2 km – i.e., the error arising from this source does not exceed one pixel. For actual relief changes error values turn out to be still lower.

At the early stages of strips pre-processing the additional phase correction was performed interactively by the operator. For this purpose he drew on the strip image a line relating to the middle of the dark zone. The coordinates of the points of the line were used for cyclic shift of the averaged image. As this procedure was extremely labourious, a little later we began to use an automatic correction procedure. Manual correction was then used only for image areas where the automatic algorithm lost its efficiency. The automatic correction was carried out by determining the maximum of the correlation function of the averaged image lines and the reference signal whose shape was determined by antenna diagram. The mean value of the video signal was first calculated from $2k + 1$ strip lines (in fact $k = 31$): i.e.,

$$\bar{x}_{ij} = \sum_{n=i-k}^{i+k} x_{nj}/2k + 1. \tag{5}$$

Then the correlation function of $\bar{x}_{ij}$ and the reference signal $f(j)$ was estimated from

$$F_{in} = \sum_{j=0}^{63} f(j)\bar{x}_{i,(j+n)_{\mathrm{mod}\,63}}, \tag{6}$$

and the maximum point m,

$$F_{im} = \max_{0 \leq n \leq 62} F_{in} \tag{7}$$

was found. The value of m was considered to be the beginning of the line i, and all elements of this line were cyclically shifted leftward by m positions.

Upon the completion of the phase increment correction the strip image was packed in the vertical fragment with 1024 lines by 252 elements. Four strips processed this way formed an image that contained 1024×1024 elements (with narrow intervals between the strips). This image was transposed (rotated around the main diagonal). As a result each of four strips became horizontal. From the image obtained the coordinates of the beginning and the end of each strip were determined interactively. This coordinates were then written into the catalogue.

The last pre-processing step was the correction of distortions caused by the antenna diagram nonuniformity. These distortions leading to a decrease in brightness and contrast at the strip edges were compensated by dividing the value of pixel

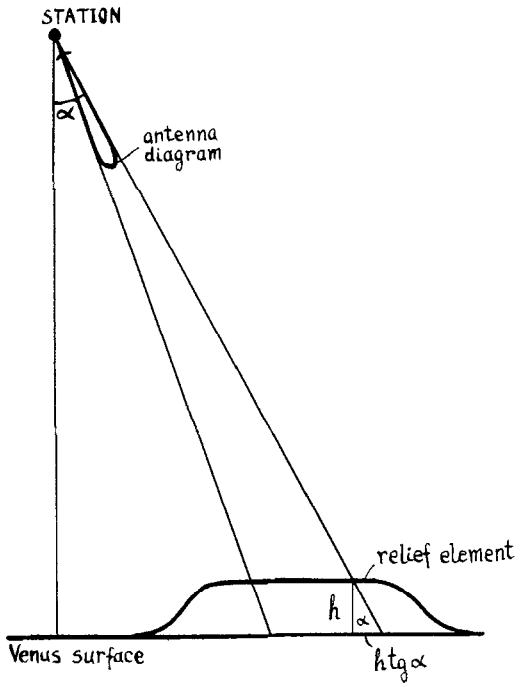

Fig. 6. The shift of the minimum of antenna sensitivity caused by Venus relief.

brightness by its current mean value along the horizontal neighbourhood with the width of 63 pixels: i.e.,

$$y_{ij} = cx_{ij} \Big/ \left(\sum_{k=-31}^{31} x_{i+k,j}/63 \right). \tag{8}$$

The average brightness of the image obtained (Figure 5e) became equal to $c = 128$ – the middle of the range for 8-bit brightness values. Text comments (serial and identification numbers and the date of obtaining each strip) were drawn on all the resulted images. Then these iamges (Figure 5f) were recorded on magnetic tapes.

3. Geometrical Transformation of Strips and Sectors Synthesis

3.1. Geometrical transformation of strips

The images of the strips had quite arbitrary geometry after pre-processing described in Section 2. In fact, since the station height varied greatly (from 1000–2000 km) in the time of location the surveyed surface area was curved. Near the pericentre, where the height was minimal, the strip approached most closely the subsatellite line (see Figure 7a). The lines were formed in equal time intervals $\Delta t = 0.296$ s. Hence, the distance on the surface between neighbouring lines was greater near the pericentre, where the station speed was maximal, and decreased towards the ends of the strip. As it will be shown below, the distances on the surface between the elements of each line were unequal too.

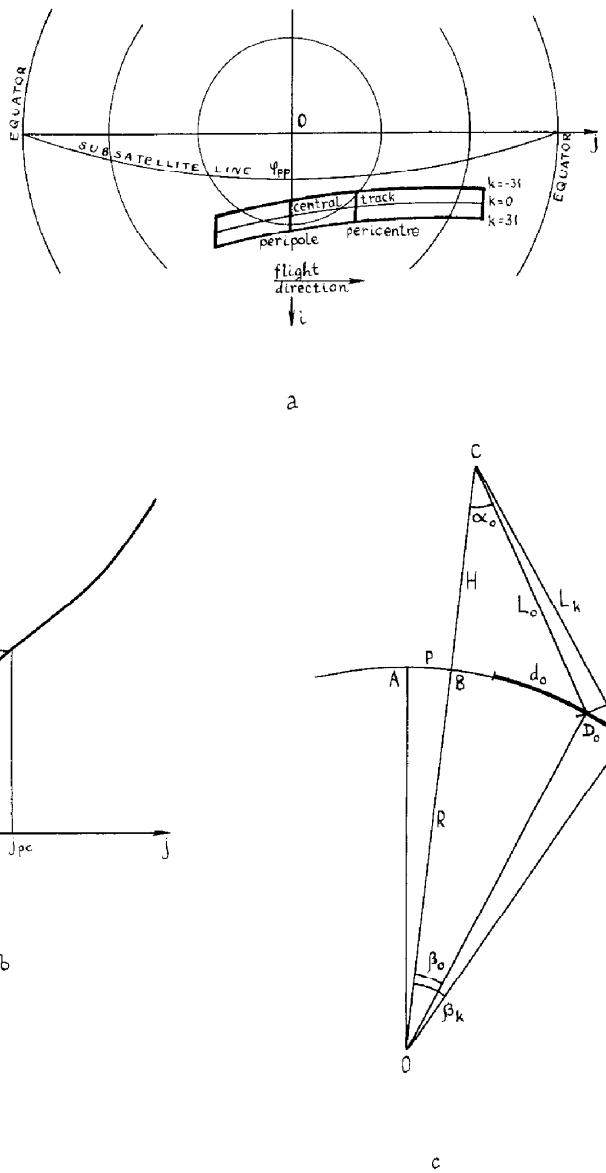

Fig. 7. Geometrical transformation of strips: a – the position of the subsatellite line, the strip and its characteristic elements on the map; b – graph of dependence of the coordinate j on the map and the number of corresponding strip line r; c – the evaluation of transverse strip deformation.

To obtain the correct strip image it was necessary to carry out appropriate geometrical transformation. The strip was immediately transformed into the map projection. So one had to take into account that the map scale along parallels changed depending on the distance from the pole and that the subsatellite line was not straight in the projection used.

Exact calculations by formulae taking into consideration all these factors call for considerable expenditures of CPU time. However, accuracy requirements are not high during the transformation of strips because the error must only be within one pixel. That is why the problem of this transformation can be radically simplified.

Figure 7a presents the image of the strip transformed to the map projection; (i, j) are coordinates of the elements of this image, (0, 0) – the element corresponding to the pole. The horizontal axis of this image ($i = 0$) is a meridian along that the station is flying.

The lines of the transformed strip must be perpendicular to the subsatellite line. However, for real orbital prameters the deviation of the points of this line from the meridian in the projection chosen is very small, and the strip lines can be regarded as perpendicular to the meridian. Only the coordinate j can therefore be used in calculating the station height H and in carrying out the longitudinal strip extension. Denoting the pericentre coordinate by j_{pc}, let us introduce designations for two angles

$$\varphi(j) = \frac{\mu}{R} j \quad \text{and} \quad \psi(j) = \frac{\mu}{R}(j - j_{pc}), \tag{9}$$

where $\mu = 2.5$ km/pixel – the map scale (the size of an element along the meridian), $R = 1051$ km – radius of Venus. φ is the angular size of the arc between the pole and the point of the meridian (the latitude of that point is equal to $90° - |\varphi|$), ψ is the angle entering the equation of the station orbit. The graph in Figure 7b illustrates the extension of the strip, i.e. the dependence between the coordinate j and the number of the corresponding strip line r. Note that the values of r_{pp} and r_{pc} (numbers of the lines corresponding to the peripole and the pericentre) for the strip being transformed are known from the catalogue, and j_{pc} is *a priori* unknown.

To perform the longitudinal extension, an array

$$S_n = \sum_{k=1}^{n} \frac{\mu H_{pc}(1 + e)^2}{R V_{pc} \Delta t (1 + e \cos(k\mu/R))^2} \tag{10}$$

was formed; where H_{pc} denotes the station height in the pericentre taken from the catalogue, while V_{pc} and e stand for the station's speed in the pericentre and the eccentricity of its orbit in the given cirucit. They were calculated from the equations

$$V_{pc} = \sqrt{(D/H_{pc}) + E}, \qquad e = 1 + 2EH_{pc}/D, \tag{11}$$

where $D = 2\gamma m_v$ (γ = gravitational constant, m_v = mass of Venus). $E < 0$ was the parameter written in the catalogue – full energy of the station element with the mass of 2 g. The coordinate j_{pc} was then determined from the condition

$$S(j_{pc}) = r_{pc} - r_{pp}, \tag{12}$$

and the longitudinal extension was fulfilled by the formula

$$r(j) = r_{pc} + S(|j - j_{pc}|)\ \text{sign}(j - j_{pc}). \tag{13}$$

Let us now describe the transverse deformation of the strip (along its lines). So far we shall not take into account the change in the map scale. Let us estimate all the distances in kilometers on the surface in the direction perpendicular to the meridian (Figure 7c). For the given coordinate j the deviation of the subsatellite line from the meridian $p = R\varphi_{pp} \cos \varphi(j)$ (the value of φ_{pp} is known from the catalogue). The station height over the surface is

$$H = (R + H_{pc}) \frac{1 + e}{1 + e \cos \psi} - R. \tag{14}$$

Let, moreover, k denote the number of the element of the strip line relating to the coordinate j ($-31 \leqslant k \leqslant 31$); D_k, the surface point corresponding to this element; β_k, the angle BOD_k (Figure 7c); and L_k, the distance from the point D_k to the station. After determining the angle

$$\beta_0 = \arcsin\left(\frac{R + H}{R} \sin \alpha_0\right) - \alpha_0, \tag{15}$$

where $\alpha_0 = 10° -$ the inclination angle of the side-looking radar – one can find the distance from the considered point of the central track of the strip (connecting elements with $k = 0$) to the subsatellite line $\mathrm{d}_0 = R\beta_0$ and the distance between this point and the station $L_0 = R \sin \beta_0 / \sin \alpha_0$. The distance from the station to the arbitrary point D_k of the same strip line is $L_k = L_0 + k\Delta L$, where $\Delta L = 0.462$ km. The use of the formula

$$\beta_k = 2\arcsin\left(\left(\sqrt{\sin^2 \frac{\beta_0}{2} + 2L_0 k \Delta L + (k\Delta L)^2}\right) \Big/ 4R(r + H)\right) \tag{16}$$

gives the possibility to calculate the deviation of the point D_k from the subsatellite point, $d_k = R\beta_k$.

Calculations by formulae (15) and (16) take much time. That is why in practice the values of d_k were determined somewhat differently. It can be shown that the deviation of the point from the central track of the strip $\Delta d_k = d_k - d_0 = R(\beta_k - \beta_0)$ varies slowly with the change of the height H. Therefore, tables common for all the strips were compiled. They contained values of $\Delta \mathrm{d}_k$ for various H quantized with the step of 64 km. All these tables could be easily kept in CPU memory. The values of d_0 were found quickly and with enough accuracy after approximating the dependence $\mathrm{d}_0(\mathrm{H})$ by a second-degree polynomial.

Thus, the deviation of the element from the meridian, expressed in kilometers, was calculated as a sum of three components: the deviation of the subsatellite point from the meridian, the deviation of the central track point from the subsatellite line, and the deviation of the current element from the central track.

Let us see now how the image of the transformed strip was formed. For each of its column, i.e., for the given j, the number $r(j)$ of the corresponding line of the pre-processed strip was determined, values of φ, ψ, and H were calculated and from the quantized value of H the table with the values of $\Delta \mathrm{d}_k$ was found. The deviation

of the subsatellite line from the meridian p and the deviation of central track from the subsatellite line d_0 were calculated too. Then, with the account of scale nonuniformity, the distance (in kilometers) of each element (i, j) from the meridian $\rho = i\mu \sin \varphi/\varphi$ was determined, and the value of Δd_k was found from the equation

$$\rho = p + d_0 + \Delta d_k. \tag{17}$$

The number of element k that corresponded to this value was taken from the table. The brightness of the element of the preprocessed strip with coordinates (r, k) was finally addressed to the element (i, j) of the transformed strip.

The result of geometrical transformation is shown in Figure 8a. Note that the bend of the strip due to its deviation from the subsatellite line is almost compensated by the bend of the subsatellite line. The strip narrowing at the ends is compensated by the extension due to the change in the scale. Each line of the strip is nevertheless nonlinearly extended; this nonlinearity is especially high near the pericentre.

3.2. Sector synthesis

The geometrical transformation described above restores quite accurately the shape of the strip, but does not determine its exact position due to the use of approximate values of initial data. For instance, a small error in the peripole coordinate r_{pp} leads to the corresponding shift of the entire strip, although practically leaves its shape unchanged. Therefore, in further work with the map neighbouring strips were referred to objects on them.

In principle, one could refer the second strip to the first one, synthetize the common image of two strips, refer the next strip to it, and so on. However, when the circuit is closed, the last strip will not coincide exactly with the first one due to accumulation of errors in the turn angles and shifts. It is also clear that any strip reference error would require a revision of the results of entire subsequent work. There are also some technological considerations that compel us to reject this method; the main of them being the limited size of the magnetic discs.

Therefore, the intermediate stage of operation was introduced – the synthesis of map sectors (Figure 8). The map was divided into 19 sectors (see Figure 4); each of them comprised up to 16 strips and covered 15–20° on the surface. The neighbouring sectors had a common strip: the last strip of each sector was in the same time the first strip of the next sector. The size of the sector was determined by the size of the magnetic discs.

The synthesis of each sector began with the geometrical transformation of the base strip. Upon being transformed, this strip directly (without the turn) became the initial part of the sector. Then the neighbouring strip was transformed and referred to the base one by turn and shift.

The determination of turn and shift values was carried out interactively. Two corresponding objects were found for this purpose in both strip images: one in the peripolar area (i.e. in the area of the maximum overlap) and another one in the area lying 3000–4000 km from the peripole (where the appropriate strips overlap still

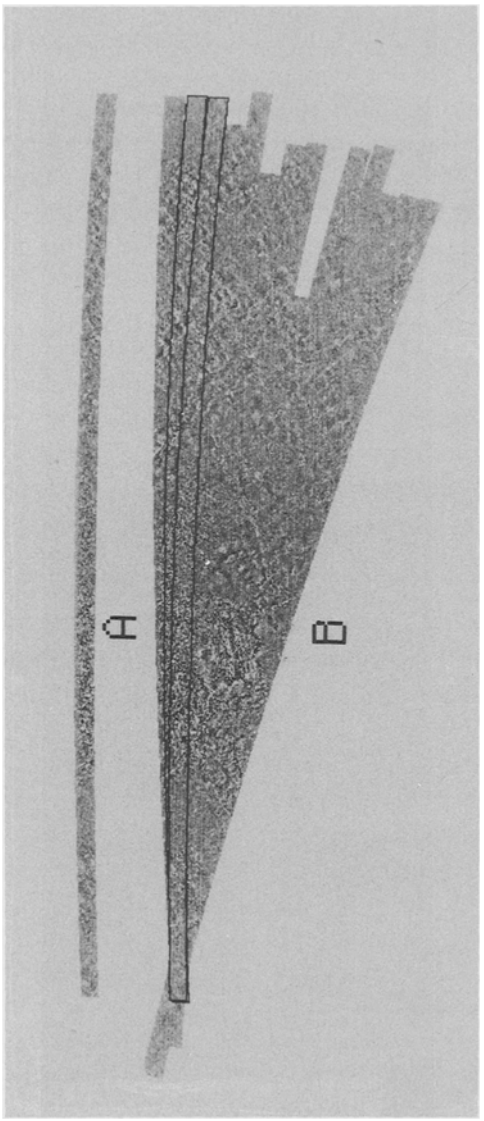

Fig. 8. a – the neighbouring strip after the geometrical transformation; b – the result of sector synthesis (contours of base and neighbouring strips are outlined).

occurred). At first the position of these objects was roughly shown by placing marks on them at the full strip images on the display processor screen. For the subsequent exact objects referencing we took a chance of storing simultaneously – in the display processor memory – two image fragments and of instantaneous transition from the displaying of one fragment to the displaying of another one and vice versa (after pushing or releasing a button). This enables one to compare the fragments very effectively, provided they have the same scale and orientation. In the course of referencing the images of both above-mentioned areas for both strips were read from the disc to the CPU memory; two areas corresponding to the same object (the area of the base strip and the area of the neighbouring strip subjected to the turn and the shift in accordance with the current parameters values, Figure 9) were then transferred to the display processor memory. The images of both areas could be shifted to achieve the co-incidence of their centres with the chosen object and the optimal correspondence of this and other objects on the base and neighbouring strips. The comparison parameters (coordinates of areas centres, scale factor and turn angle, see Figure 9) were also reproduced on the display processor screen

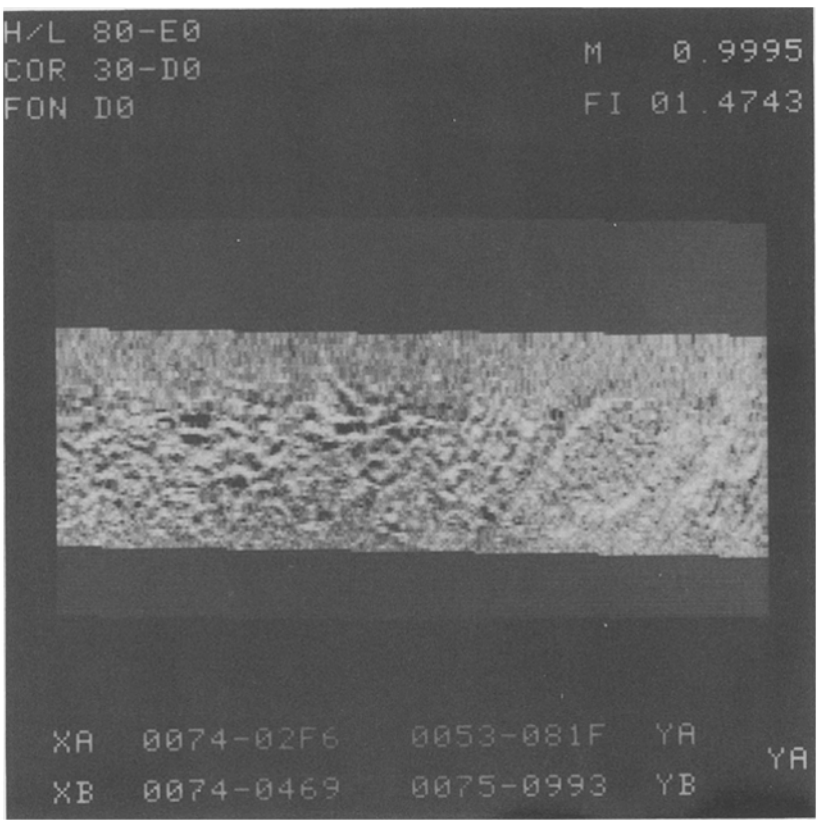

Figure 9(a).

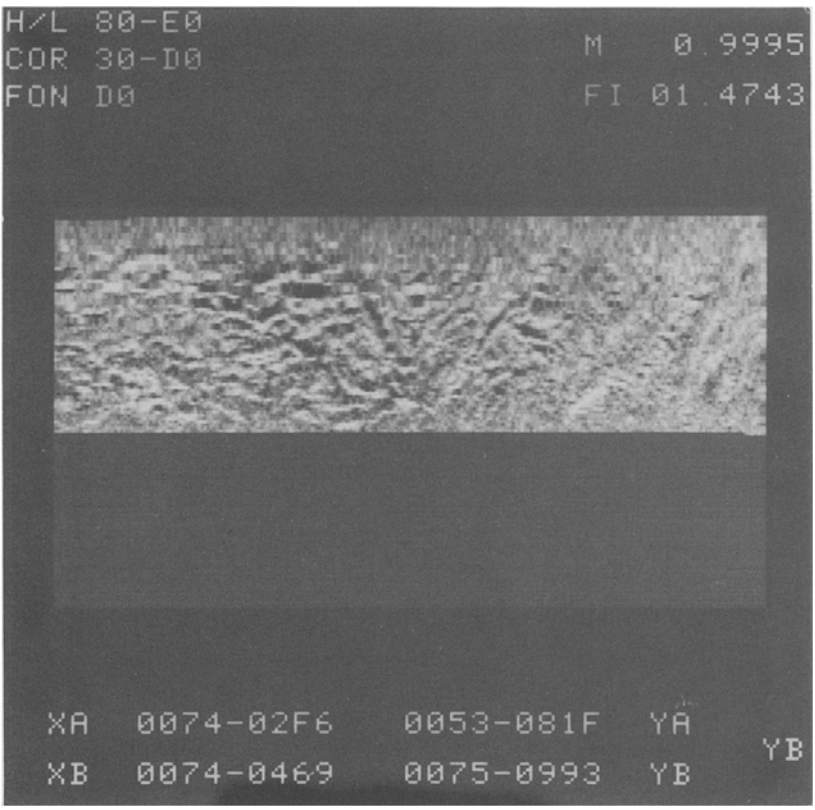

Figure 9(b).

Fig. 9. The referencing of base and neighbouring strips: a – a fragment of neighbouring strip image after shift and turn; b – a fragment of base strip.

during the operation. This enabled the additional control of the correctness of strips superposition: the final turn angle must be close to 1.48°, and the scale must be approximately 1.

Upon completion of the referencing, its parameters were automatically written in the corresponding section of sectors catalogue (in the same way as the parameters of the base strip at the beginning of work with the sector), and the geometrical transformation of the whole neighbouring strip was performed. Irrespective of the parameters found, this transformation was carried out with the scale of 1, i.e., the images were aligned with respect to the first reference point (in the peripolar area), and the neighbouring strip was turned, while the second reference point was used only for determining the turn angle.

Upon completion of the referencing and the geometrical transformation the joint image was formed from the base and the neighbouring strips. Special interactive 'cut-in' procedure was used for this purpose. The enlarged parts of both strips were presented to the operator one under the other on the display processor screen.

Using display processor buttons, the operator could draw a broken line simultaneously in both corresponding areas, fixing the breakpoints of this line (see Figure 10). Upon reaching the edge of the screen, the images were automatically shifted in proper direction (by 1/8 of the screen upward or downward and by 1/2 of the screen to the left or to the right). The broken line segments getting into the new area were preserved on the image. The broken line was the separation boundary between the strips. The operator did his best to draw this line so that the regions of strips lying on the different sides of the line would have close brightness, and would be relatively uniform and similiar in texture. (In particular, it was recommended that the line should be drawn in valleys or along ridges, bypassing isolated craters.) If a part of the line was drawn inadequately, the operator could consecutively cancel the choice of the arbitrary number of line segments and then, beginning with a certain place, choose another route or refine the route chosen earlier.

After drawing the broken line along the entire intersection region of both strips, the operator surrounded by it the end of the neighbouring strip and connected (by pushing an additional button) the last point of the line with its initial point. Then the outlined zone of the base strip was automatically replaced by the same zone of

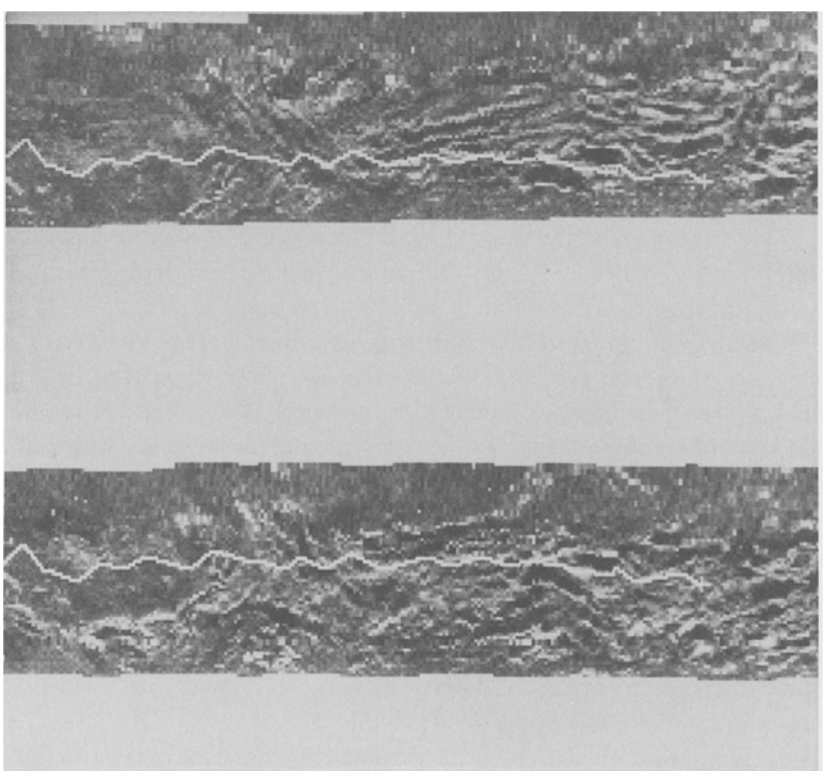

Fig. 10. The 'cut-in' procedure (photograph from the display processor screen).

the neighbouring strip. In the case of drawing the line carefully the border between two parts of the image obtained was invisible.

The choice of the strips preprocessing method described in Section 2 that excludes the appearance of strips elements with zero brightness made it possible to construct the cutting-in procedure so that zero values would not be re-recorded onto the base image. This ensured the re-recording of only the content-bearing part of the neighbouring strip image.

Upon completion of strip cutting in the image obtained was made the base one, and then the procedures of geometrical transformation, referencing, turn and cutting in were repeated for the next strip. This process continued until the full sector was formed out of 10–16 strips. The sector length (see Figure 8b) was about 3000 pixels; its height was about 1000 pixels in the widest part.

4. Map Formation

The first stage of the map formation was to determine the positions of the sectors on the map from *a priori* data and the results of sectors synthesis. The sector catalogue contained for each sector s the angles θ_s and η_s of the turn of its upper and lower strip with respect to the meridian. Since the upper strip of sector s was in the same time the lower strip of sector $s+1$ (see Figure 4a) it was possible first of all to determine the overall angle embraced by all 19 sectors

$$\gamma_0 = \sum_{s=1}^{19} (\eta_s - \theta_s). \tag{18}$$

Due to the limited accuracy of strips preprocessing and sectors synthesis and due to the discretization error the angle γ_0 was equal not to 360°, but only to 355.6°. Therefore, in the course of map formation each sector had to be extended $M = 360/\gamma_0$ times, i.e., approximately by 1% of its angular size.

The general orientation of the map was determined from the coordinates of characteristic object of the first sector – the so-called Cleopatra Patera (these coordinates were known from independent sources). The longitude of this object assigned the turn angle of the first sector, γ_1, and its latitude – the shift of this sector. The turn angles of the remaining sectors were determined by the formula

$$\gamma_s = \gamma_1 + M \sum_{k=2}^{s} (\eta_k - \theta_{k-1}). \tag{19}$$

The errors in determining the peripole coordinates in the course of the geometrical transformations of the sectors base strips resulted in the shift of the sectors. In the course of the map formation it was necessary to compensate this shift so that the turn around the pole would lead to the coincidence of the outer strips of neighbouring sectors. To determine the shift parameters we measured the coordinates of two corners of the right-hand ends of the upper and lower strips of each sector (points A_s, A'_s, B_s, and B'_s, respectively). The coordinates of the points B_s and

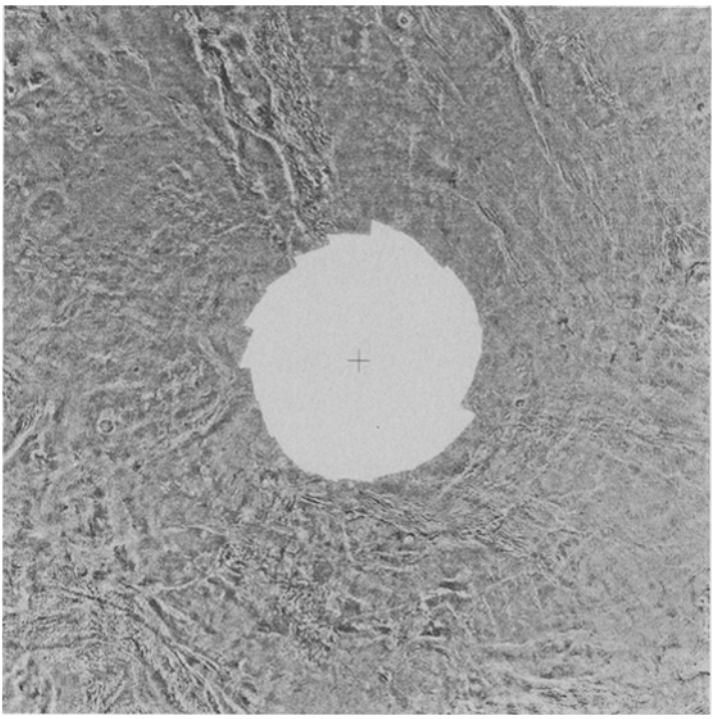

Figure 11(a)

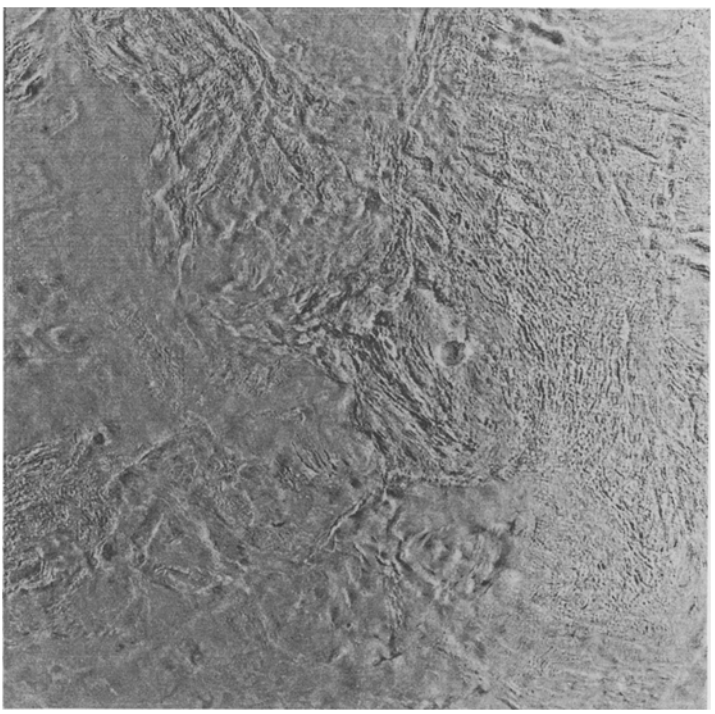

Figure 11(b).

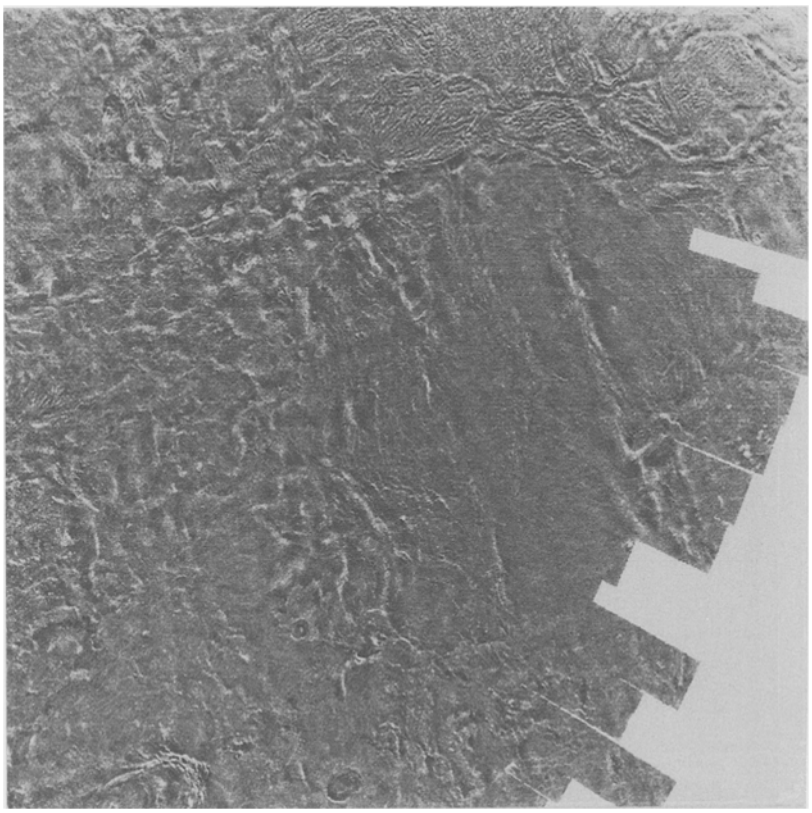

Figure 11(c).

Fig. 11. The sheets of the map: a – central sheet (with polar area empty); b – one of middle sheets; c – one of peripheral sheets.

B'_s were recalculated into the coordinate system of the sector $s-1$ by turn at the angle $M(\eta_s - \theta_{s-1})$ counter-clockwise. After this the average non-coincidence of the coordinates obtained with the coordinates of points A_{s-1} and A'_{s-1} was taken as the shift of the sector s with respect to the sector $s-1$.

The calculation of the shift and turn parameters for sectors 2–19 enabled us to find the absolute shift parameters of each sector on the map. As it was expected, upon the completion of this procedure the outer strips of sectors 19 and 1 did not coincide, but were shifted with respect to each other. The shift magnitude was only 7 pixels; this, as well as the insignificant error of the total turn angle γ_0, testified to the correctness of the chosen method of map formation. For shift compensation the correction (by one pixel) of the relative shifts of some sectors were done.

After determining the sectors turn and shift parameters the map formation process was begun. Due to the limited volume of magnetic discs available the map was formed from separate sheets. It comprised 49 sheets, of which only 34 sheets contained information; the size of each sheet was 1024 × 1024 pixels (see Figure 3).

Each sector included in the formed sheet was first extended M times. In practice the angular extension was replaced by linear extension in accordance with the formulae,

$$\begin{cases} i' = i_0 + (i - i_0) \sin M\delta_0 / \sin \delta_0, \\ j' = j - (i - i_0)(\cos \delta_0 - \cos M\delta_0)/\sin \delta_0, \end{cases} \tag{20}$$

where i_0 is the average distance from the meridian ($i = 0$) to the end of the upper strip of the sector, and $\delta_0 = 19°$, the average sector covering angle. The error occurred was less than one element everywhere on the sector. After the extension the sector was shifted and turned, taking into account the position of the sheet on the map.

To join the parts of sectors comprising each sheet we used the 'cut-in' procedure similiar to that described in Section 2. Enlarged fragments of the images of the sheet and the sector situated one under the other were presented to the operator, and he drew a broken line on these images with the method described above. Upon closing the ends of the broken line the content-bearing part of the sector, limited by this line, was cut in the image of the sheet. Extension, shift, turn, and cutting-in of the sectors continued until information from all sectors comprising a sheet was put onto it (Figure 11).

5. Polar Area Filling

The central sheet of the map obtained after joining the sectors had a gap in the polar area (Figure 11a). To fill this gap one of the stations was turned by 20° around its longitudinal axis approximately once a week or two; in this case the strips surveyed by the station radar passed through the pole (Bogomolov *et al.*, 1985).

The geometrical transformation of polar strips did not differ in principle from the above-mentioned transformation of ordinary strips. It was carried out by the same formulae but in a specific operation mode: the inclination angle of the radar $\alpha_0 = 10°$ was replaced by $\alpha_p = -10°$. The shift of the image field coordinates was also ensured so that the strip transformed would get into this field. Since polar strips lay higher than the subsatellite line the bend of the subsatellite line and the deviation of the central track from the subsatellite line complemented each other. As a result, the polar strips transformed into the map projection were much more curved than the ordinary strips.

The information about station flight trajectory in the days of polar strips survey was, as a rule, inaccurate, and only the approximate value of the station turn angle α_p was known. It was therefore decided to refer these strips to the central sheet of the map with checking the turn angle (determined by the survey date), but without preserving the unit scale (i.e., with possible increase or decrease of the strip). The referencing was performed not for the entire strip, but only for its central part with the length of about 1000 pixels. Venus North pole lay approximately in the middle of this part. The interactive referencing procedure similar to that used to synthetize

the sectors consisted in searching – on the central sheet of the map – objects corresponding to the objects at the beginning and at the end of the polar strip turned by the angle close to the theoretical one. The operator shifted the enlarged images of the strip fragments and/or of the central sheet fragments until the chosen objects (and also the objects located nearby) coincided. The plausibility of the turn angle and the closeness of the scale to unity were the criteria of the correctness of referencing. Upon its completion the central part of the strip was turned and shifted so that the chosen objects coincided. Then the cutting of the strip in the central sheet of the map was performed (Figure 12a). The process of geometrical transformation, referencing, shift, turn, and cutting-in of the polar strips continued until the filling of the polar area gap (Figure 12b). For each next strip the referencing was, as a rule, simpler and more accurate since it could be checked up by the coincidence of the objects located in the polar area. For all the polar strips the turn angles obtained were close to theoretical ones, and the scale was always within 1 ± 0.005. Thus, despite rough assumptions, the chosen technique has proved to be quite acceptable.

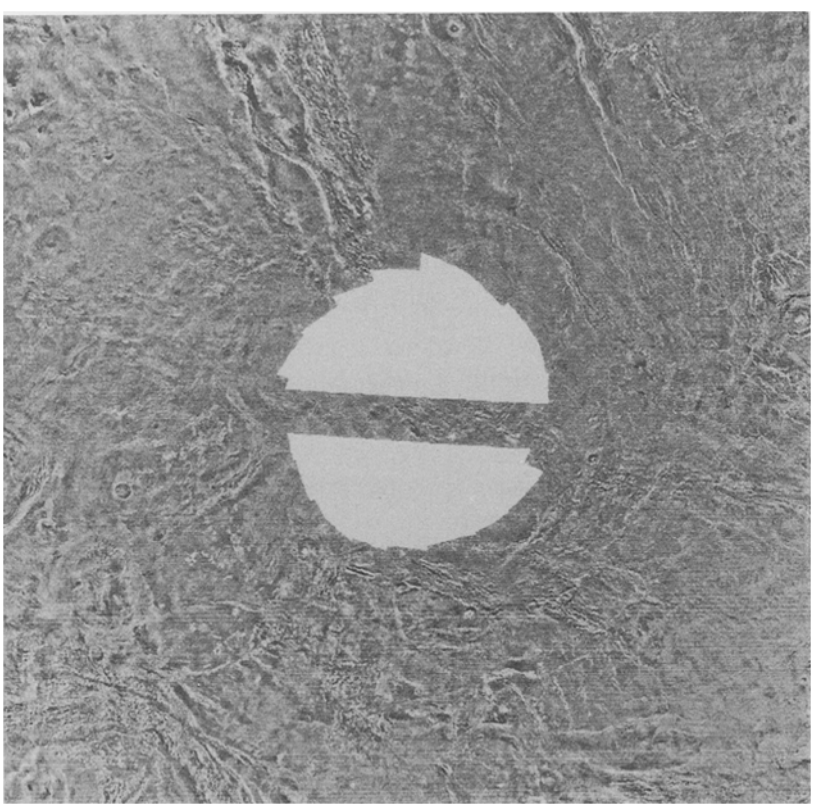

Figure 12(a).

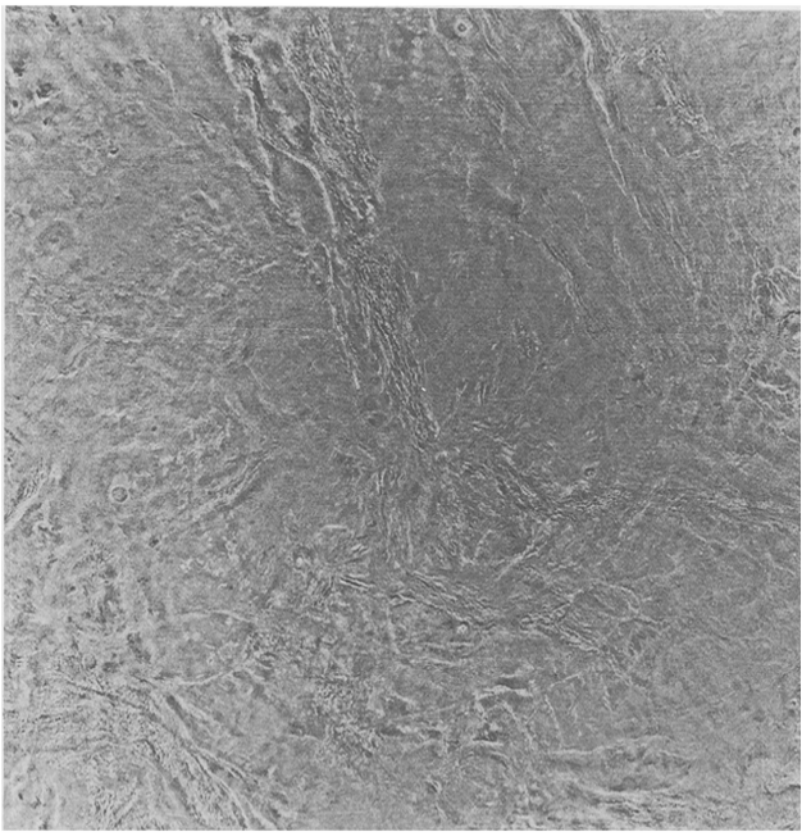

Figure 12(b).

Fig. 12. Polar area filling: a – central sheet of the map with one 'polar' strip attached; b – central sheet with polar area filled.

6. Conclusion

The above-described methodology enabled us to complete successfully the synthesis map of Venus (Figure 13). Within a relatively short time the images of about 300 strips were processed, 19 sectors were synthesized from these images, 34 sheets of the map were formed from the sectors, and the polar area of the central sheet of the map was filled with polar strips. A specific feature of the methodology used was the extensive application of interactive image processing methods. Thanks to this the quality of the images was sharply enhanced, the borders between neighbouring strips and sectors were made indistinguishable, and high accuracy of geometrical transformation was ensured. The rational technique of strips preprocessing, sectors synthesis, and map formation has made it possible to lower the requirements to professional training of the operator and to work with rather high speed.

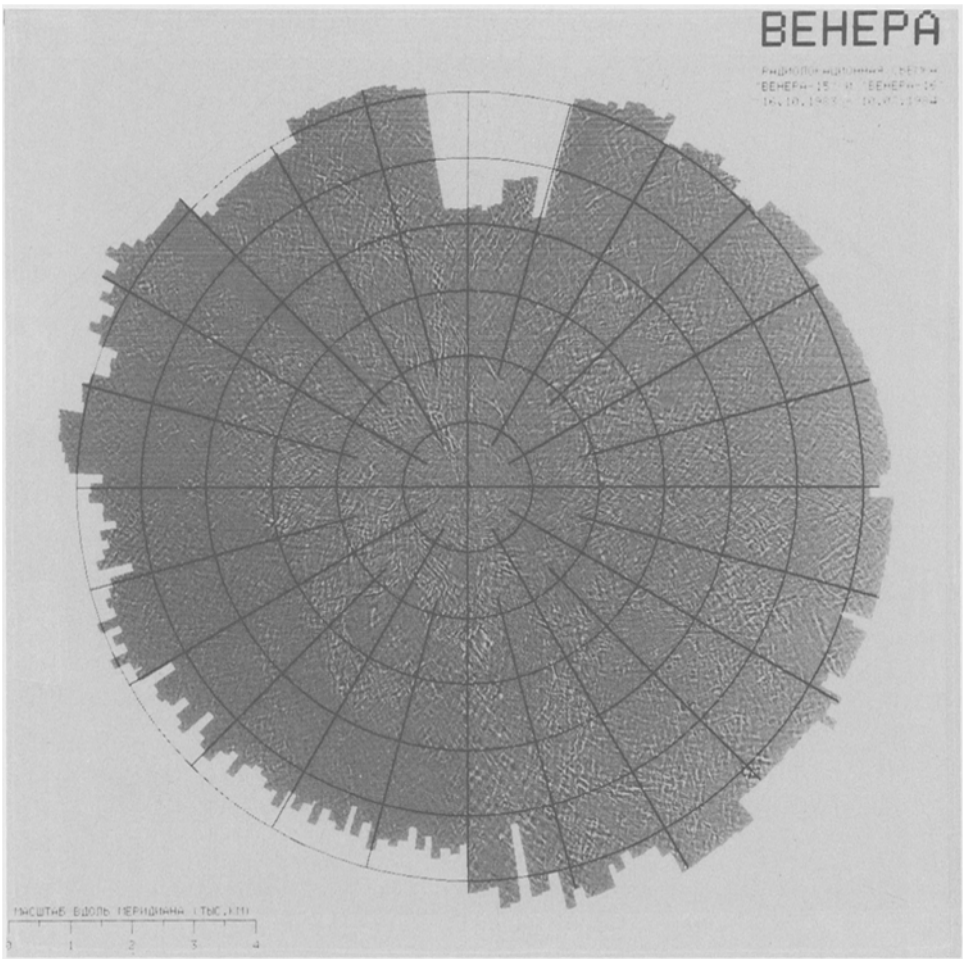

Fig. 13. The entire radiolocation map composed from the results of Venus strip survey.

Acknowledgements

The authors are thankful to the Moscow Energy Institute for presenting the initial data of the strip survey and the information about flight orbits. Thanks are also due to N. I. Zasolova and L. V. Kudrin for their participation in the practical work of map synthesis.

References

Akim, E. L. *et al.*: 1986, 'The Navigational Aspect and the Fixation of the Data of the Radar Survey from Veneras 15 and 16'. *Geodesiya i kartografiya* (*Geodesy and Cartography*), No. 1, pp. 38–41.

Bogomolov, A. F., Skrypnik, G. I., Bockstein, I. M., Kronrod, M. A., Chochia, P. A. Bergman, M. U., Kudrin, L. V., and Bashnin, A. V.: 1985, 'Processing of Venera 15 and Venera 16 data of Venus Surface Strip Survey', *Kosmicheskiye issledovaniya* (*Space researches*) **XXIII**, no. 2, pp. 179–190.

Bockstein, I. M.: 1981, 'The Display Processor for Interactive Processing of Greyscale Images'. In *Cifrovaya obrabotka signalov i ee primeneniya* (*Digital Signal Processing and Its Applications*), Nauka Publishers, Moscow, pp. 187–206.

Kronrod, M. A. and Chochia, P. A.: 1983, 'Software for Interactive Image Processing System'. In *Ikonika. Teoriya i metody obrabotki isobrazseniy* (*Iconics. Theory and Methods of Image Processing*), Nauka Publishers, Moscow, pp. 87–99.

Kuzmin, R. O., Burba, G. A., Shashkina, V. P., Bogomolov, A. F., Gerichin, N. V., Skrypnik, G. I., Kudrin, L. V., Bergman, M. V., Rzsiga, O. N., Sidorenko, A. I., Alexandrov, U. N., Bockstein, I. M., and Kronrod, M. A.: 1986, 'The Relief and Geology of Venus North Pole Area'. *Astronomicheskiy vestnik* (*News of Astronomy*) **19**, No. 3, pp. 177–195.